



High Temperature Tensile Properties of Unidirectional Hi-Nicalon/Celsian Composites In Air

John Z. Gyekenyesi
Ohio Aerospace Institute, Brook Park, Ohio

Narottam P. Bansal
Glenn Research Center, Cleveland, Ohio

National Aeronautics and
Space Administration

Glenn Research Center

Acknowledgments

The authors are grateful to Mr. John A. Setlock of Case Western Reserve University (CWRU) for his assistance with composite processing and microstructure analysis.

This report is a formal draft or working paper, intended to solicit comments and ideas from a technical peer group.

This report contains preliminary findings, subject to revision as analysis proceeds.

Trade names or manufacturers' names are used in this report for identification only. This usage does not constitute an official endorsement, either expressed or implied, by the National Aeronautics and Space Administration.

Available from

NASA Center for Aerospace Information
7121 Standard Drive
Hanover, MD 21076
Price Code: A03

National Technical Information Service
5285 Port Royal Road
Springfield, VA 22100
Price Code: A03

HIGH TEMPERATURE TENSILE PROPERTIES OF UNIDIRECTIONAL HI-NICALON/CELSIAN COMPOSITES IN AIR

John Z. Gyekenyesi
Ohio Aerospace Institute
Brook Park, Ohio 44142

Narottam P. Bansal
National Aeronautics and Space Administration
Glenn Research Center
Cleveland, Ohio 44135

SUMMARY

High temperature tensile properties of unidirectional BN/SiC-coated Hi-Nicalon SiC fiber reinforced celsian matrix composites have been measured from room temperature to 1200°C (2190°F) in air. Young's modulus, the first matrix cracking stress, and the ultimate strength decreased from room temperature to 1200°C (2190°F). The applicability of various micromechanical models, in predicting room temperature values of various mechanical properties for this CMC, has also been investigated. The simple rule of mixtures produced an accurate estimate of the primary composite modulus. The first matrix cracking stress estimated from ACK theory was in good agreement with the experimental value. The modified fiber bundle failure theory of Evans gave a good estimate of the ultimate strength.

1. INTRODUCTION

Ceramics in general are extremely brittle, have low strain tolerance, and exhibit a wide variation in ultimate strength. The observed scatter in strength is caused by an abundance of imperfections, i.e., flaws that are a result of material processing. Over the years, the strength reliability of monolithic ceramics has improved as better processing techniques have evolved. However, the brittle failure characteristics of these materials make them acceptable in only a limited range of applications. In an effort to increase ceramic toughness and strength, ceramic matrix composites (CMCs) with various reinforcements are being developed. These developments are covered briefly by King (1989) and Levine (1992). These composites may include multiple phases or matrices with particulates, whiskers, or continuous fibers.

In the gas turbine industry, CMCs are particularly attractive since they have the potential to replace nickel base superalloys in various hot section components [Dix and Petty (1990) and Constance (1990)]. The primary attribute of CMCs relative to nickel-base superalloys is the ability of CMCs to be used well beyond current turbine service temperatures, as well as to withstand more severe operating environments. This would enable engines to be operated at higher temperatures with near-stoichiometric combustion without cooling air requirement penalties as noted by Drascovich (1993). Increasing operating temperature is a classic approach for improving turbine efficiency. Zweben (1998) notes that the low density and high temperature properties of CMCs make them potential materials in hot structures and propulsion systems of reusable launch vehicles.

Another attraction of ceramic composites is their relatively low density, which is, as Holmes and Wu (1995) point out, typically 65% to 75% lower than conventional superalloys. One can not overemphasize the fact that weight is a critical design facet for turbines utilized in aerospace propulsion. Lastly, CMCs offer the potential of increased durability, relative to superalloys, at the high operating temperatures. This would result in increased time between engine overhauls and reduced operating costs.

In virtually all ceramic matrix composite systems the goal of the materials scientist is to apply a closing pressure on existing matrix crack surfaces and to impart a tortuous fracture path by crack deflection. This results in an increase in the apparent toughness of the material as noted by Warren (1992). Unlike polymer and metal matrix composites, the fiber/matrix interface in a fiber reinforced ceramic composite must be relatively weak. Optimization of the interface prevents matrix cracks from propagating through the fibers while still providing load transfer. As a result, unbroken fibers bridge a propagating matrix crack, which increases the composite work of fracture. In

essence, the fiber/matrix interface has to be strong enough to allow load transfer and retain acceptable strength in the transverse direction, but the interface must also allow debonding as a crack passes around the fiber.

There are many ceramic matrix composite systems being investigated and developed, as indicated by Sheppard (1992) and Studt (1991). One of these systems consists of boron nitride and silicon carbide coated silicon carbide fibers and a strontium barium aluminosilicate (celsian) matrix. As an oxide, the matrix doesn't have the oxidation problems of silicon based ceramics.

The path to successful commercialization of the CMC systems mentioned above must include the characterization and evaluation of engineering design properties. As Duffy and Gyekenyesi (1995) point out, this requires characterization of mechanical and thermal properties. It is essential to characterize the creep behavior of these materials as well as to ascertain how temperature affects their fast fracture. Motivated by the general lack of high quality test data required by the design engineer, this paper presents high-temperature, fast fracture data of the aforementioned SiC/Celsian composite. This data was acquired using a high temperature tensile testing facility assembled by Gyekenyesi (1998) at NASA Glenn Research Center. The properties of these material systems were obtained in the primary fiber direction.

Strong and tough celsian matrix composites reinforced with large, $\sim 140\text{ }\mu\text{m}$, [Bansal (1993, 1994, and 1996)] and small, $\sim 14\text{ }\mu\text{m}$, diameter [Bansal (1997) and Bansal et al. (1995 and 1998)] silicon carbide fibers have been described earlier. The main objective of this study was to evaluate the high temperature mechanical behavior of a SiC/celsian composite in an oxidizing environment. Another objective was to test the applicability of currently available micromechanical models in predicting the values of modulus, proportional limit or first matrix cracking stress, and ultimate strength for these composites.

2. MATERIALS

Polymer derived Hi-Nicalon™ SiC fiber tows (1800 denier, 500 filaments/tow) from Nippon Carbon Company, Ltd. were used as the reinforcement. A dual layer of BN and SiC was applied on the fibers by Minnesota Mining & Manufacturing (3M) using a continuous chemical vapor deposition (CVD) reactor. The nominal coating thicknesses were $0.4\text{ }\mu\text{m}$ ($16\text{ }\mu\text{in.}$) for BN, and $0.3\text{ }\mu\text{m}$ ($12\text{ }\mu\text{in.}$) for SiC.

The SiC/Celsian composites were fabricated by impregnation of the fiber tows with the matrix slurry as described earlier [Bansal (1997) and Bansal and Setlock (1996)]. Unidirectional fiber reinforced composites were fabricated with 12 plies. The resulting composites were almost dense with $\sim 5\%$ porosity. The 150 mm by 150 mm (6 in. x 6 in.) fiber-reinforced composite panel was surface polished and machined into test bars with contoured gage sections for tensile testing. The bars were first cut from the panels using a diamond impregnated wheel. The contours were ground. The dimensions and geometry of the tensile test specimens, based on Worthem (1990) and Worthem and Lewinsohn (1991), are shown in Fig. 1.

3. EQUIPMENT AND TEST PROCEDURES

Details of the equipment used to tensile test flat ceramic matrix composite specimens to temperatures over 1500°C (2730°F) in air were described earlier [Gyekenyesi (1998) and Gyekenyesi & Jaskowiak (1999)]. The system consists of a universal tensile testing frame with a 50 kN load cell and rigidly mounted, water cooled, hydraulically actuated wedge grips. An alignment device is mounted in the load train between the crosshead and load cell. Axial strains in the specimens were measured by a clip-on extensometer for the room temperature tests and a low contact force mechanical extensometer for the high temperature tests. The gage lengths were fixed at 25 mm (0.98 in.). An induction heating system with a recrystallized silicon carbide susceptor was used to heat the specimen to the test temperature. Lastly, a computerized data acquisition and analysis system was used to collect and interpret the test data.

Two coupons were tested at each temperature. Tensile tests were performed at room temperature, 800, 1000, 1100, and 1200°C (1470 , 1830 , 2010 , and 2190°F) in air in the load control mode. The loading rate was fixed at 1.0 kN/min (225 lbf/min). The specimens were loaded until failure. The furnace was heated at a rate of 30°C/min (54°F/min.) and held at temperature for $\sim 5\text{ min}$ for the temperature to stabilize. Other details were presented earlier [Gyekenyesi & Jaskowiak (1999)].

The stress-strain curves were used to determine first matrix cracking stress, Young's modulus, and ultimate tensile strength. The first matrix cracking stress was assumed to occur at the proportional limit on the stress-strain curve. The elastic modulus of the composite was determined from the linear portion of the stress-strain curve. Fracture surfaces of the test specimens were observed with a scanning electron microscope (SEM) in an attempt to determine the average matrix crack spacing and other failure characteristics.

Cyclic fiber push-in tests were performed using a desktop apparatus previously described by Eldridge (1991) and Bansal and Eldridge (1998), but with the addition of a symmetrically placed pair of capacitance gauges for displacement measurements. The indenter uses a 70°-included-angle conical diamond with a 10 µm (400 µin.) diameter flat base.

4. THEORY

Considerable effort has been applied to the mathematical modeling of the mechanical behavior of ceramic matrix composites. A complete understanding of the mechanical behavior of these composites is necessary if designers are to make use of them for high temperature engine applications. Important properties include the Young's modulus, first matrix cracking stress, ultimate strength, and work of fracture from room temperature to at least 1200 °C (2190 °F).

4.1. Modulus

One of the basic properties of interest is the primary elastic modulus. The longitudinal Young's modulus of the composite is related to the matrix and fiber moduli, and their respective volume fractions by the rule of mixtures as presented in the following equation

$$E_c = V_f E_f + V_m E_m \quad (1)$$

where E is the modulus, V is the volume fraction, and subscripts c, f, and m refer to the composite, fiber, and matrix, respectively.

4.2. Matrix Cracking and Interfacial Shear Properties

In addition to studying the composite modulus, the proportional limit, in the direction of the fibers, needs to be investigated. It is assumed that the proportional limit on a stress/strain curve and the first matrix cracking stress are the same. This is a common assumption, as noted by Woodford and his associates (1993). The first matrix crack is taken by definition as the first through the cross section crack, wherein only the fibers are left to carry the total composite load. Any minor cracking within the composite before this condition or load is reached, is ignored in this definition. It is assumed that the fiber failure stress and strain are greater than the matrix failure stress and strain, respectively. The first matrix cracking stress is the onset of permanent major damage in a composite making it a critical design parameter. Shimansky (1989) describes the cracking process for CMCs with an increasing load as usually initiating with microcracks at the fiber/matrix interface or the matrix. The microcracks coalesce upon further increase in the applied load, forming major matrix cracks perpendicular to the loading axis that eventually traverse the whole composite cross-section. Once the composite matrix is saturated with cracks, the remaining fiber/matrix interface area with each matrix segment is insufficient to transfer an adequate load to cause the matrix to fracture into smaller segments.

The first matrix cracking stress is dependent on many parameters. A key parameter is the fiber/matrix interfacial shear strength. Kerans (1989) has noted that the interfacial shear strength is difficult to characterize and may vary with location. In one technique, the fiber/matrix interfacial frictional shear strength is determined from matrix crack spacing measurements in a composite that has been loaded to or near its ultimate strength. Loading a

specimen near the ultimate strength leads to matrix crack saturation. The average crack spacing for each specimen is used to determine the mean fiber/matrix interfacial frictional shear strength, τ , using the equation

$$\tau = \frac{\beta R V_m E_m \sigma_y}{2 V_f E_c x} \quad (2)$$

where $\beta = 1.337$ from Kimber and Keer (1982), R is the fiber radius, σ_y is the composite stress where matrix cracking initiates, and x is the length over which the additional load sustained by the fibers at the crack is transferred back to the matrix. This equation is derived from a summation of forces within the composite as presented by Aveston, et al. (1971). Aveston, et al. showed that the crack spacing is between x and $2x$. Kimber and Keer (1982) demonstrated analytically that the crack spacing was closer to $1.337x$. This equation is deterministic since it is assumed that the composite stress where matrix cracking initiates, that is σ_y , is constant.

Another technique for determining fiber/matrix interfacial frictional shear stress is with the use of a fiber push-in test. An estimate of frictional sliding stress, τ , can be determined using the constant shear stress model of Marshall and Oliver (1987) which includes effects of residual stresses, but does not consider fiber roughness or Poisson expansion. Values of τ can be determined by using the following relationship

$$\tau = \frac{F^2}{8\pi^2 R^3 E(u - u_0)} \quad (3)$$

where u is the fiber end displacement, u_0 is the residual fiber end displacement after unloading, F is the applied load, R is the fiber radius, and E_f is the fiber modulus.

Aveston, et al. (1971) derived an equation for predicting the composite stress where matrix cracking initiates in brittle matrix composites. This is commonly referred to as the ACK theory and the result is presented in equation 4. The parameters include the fiber/matrix interfacial shear strength τ , the matrix fracture surface energy γ_m , the fiber radius R , the constituent volume fractions V , and constituent moduli E .

$$\sigma_y = \left[\frac{12 \tau \gamma_m E_c^2 E_f V_f^2}{E_m^2 V_m R} \right]^{\frac{1}{3}} \quad (4)$$

Note that the above equation is independent of crack size. It is a discrete model that was derived using an energy balance approach. The ACK theory uses the change in energy states within the composite from just prior to matrix crack initiation to just after the crack propagates completely through the matrix. Important assumptions included are: (1) the fiber failure strain is greater than the matrix failure strain, (2) a frictional interfacial bond between the fiber and the matrix exists, and (3) the fibers can bear the load without any support from the matrix.

Another equation for predicting the first matrix cracking stress was developed by Marshall and Cox (1988) using the crack closure pressure suggested by McCartney (1987). This approach was applied by Chulya, et al. (1991) to calculate the first matrix cracking stress in SiC/RBSN. Marshall and Cox (1988) used linear elastic fracture mechanics and assumed a single crack, loaded in mode I, propagating through a semi-infinite medium. The traction from the bridging fibers was superimposed on the crack model as closing pressure. The resulting equation is similar to the ACK results. Marshall and Cox also assumed a weak frictional fiber/matrix interface with bridging fibers. The resultant equation for predicting the composite stress, where steady state matrix cracking begins within the specimen, is

$$\sigma_y = \left[\frac{6 \tau \gamma_m E_c^2 E_f V_f^2}{E_m^2 V_m R} \right]^{\frac{1}{3}} \quad (5)$$

In most composite systems there is a coefficient of thermal expansion (CTE) mismatch between the fibers and the matrix. This results in residual stresses within the composite at temperatures other than the processing

temperature. The following equation from Budiansky, et al. (1986) is used to determine the axial residual stress within the matrix:

$$\sigma_{ma} = \left(E_m \frac{\phi_2}{\phi_1} \right) \left(\frac{E_f}{E_c} \right) \left(\frac{V_f}{1 - \nu_m} \right) \epsilon_T \quad (6)$$

where:

$$\epsilon_T = (\alpha_f - \alpha_m) \Delta T \quad (7)$$

$$\Delta T = (T - T_{proc}) \quad (8)$$

$$\phi_1 = 1 - 0.5 \left(\frac{1 - 2\nu}{1 - \nu} \right) \left(1 - \frac{E_c}{E_f} \right) \quad (9)$$

$$\phi_2 = 0.5 \left(1 + \frac{E_c}{E_f} \right) \quad (10)$$

The variables α_f and α_m are the coefficients of linear thermal expansion for the fiber and matrix, respectively. The processing temperature is T_{proc} and the test temperature is T . The Poisson's ratio, ν , for the fiber and the matrix is assumed to be the same. The following equation is used to predict the composite stress for first matrix cracking while accounting for the thermally induced residual stresses.

$$\sigma_{y\alpha} = \sigma_y - \sigma_{ma} \frac{E_c}{E_m} \quad (11)$$

Danchaivijit and Shetty (1993) and Budiansky, et al. (1986) have pointed out that the ACK theory, as well as equation 5 above, lead to lower bound predictions.

4.3. Fiber Properties

As mentioned earlier, ceramic matrix composites contain fibers that have a higher failure strain than the matrix. As a result, the ultimate strength of the composite is fiber dominated. This section briefly discusses the behavior of ceramic fibers in preparation for analyzing the ultimate strength of unidirectional composites.

Most brittle materials, including ceramic fibers, show a large variation in their tensile strength. Therefore, it is appropriate to apply statistical techniques for predicting their reliability and probability of failure. Statistical analysis allows the designer to use data generated from a small sample to systematically predict the stochastic response of complex structures.

Bergman (1984) reported that the cumulative distribution function proposed by Weibull (1939) is the most useful for characterization of brittle materials. Weibull analysis is based on the weakest link theory, where failure is assumed to occur at the largest flaw within the material. It should be noted that a single flaw population and a strength that is independent of time will be assumed.

The American Society for Testing and Materials (ASTM, 1995) has a standard (Designation: C 1239-94a) utilizing the maximum likelihood technique for estimating the Weibull parameters. The maximum likelihood method will be used for this work.

The ASTM (1995) standard, designation C 1239-94a, states that the estimated Weibull modulus tends to be statistically biased. The bias decreases as the sample size is increased. The ASTM (1995) standard provides a table of unbiasing factors as a function of sample size. Other details were covered by Gyekenyesi (1998).

4.4. Ultimate Strength

The ultimate strength of the Hi Nicalon fiber reinforced celsian matrix composites is primarily dependent on fiber properties. A simple approximation for predicting the composite ultimate tensile strength utilizes the rule of mixtures and the mean fiber strength. For unidirectional lamina, assuming that the in-situ fiber and the independent fiber strengths are identical and that the matrix carries no load, we have

$$\sigma_{cu} = V_f \sigma_{fu} \quad (12)$$

where σ_{cu} is the composite ultimate strength and σ_{fu} is the mean fiber ultimate strength. It is further assumed here that all the fibers are intact until just prior to the composite ultimate loading.

The assumption of uniformly strong fibers would be the ideal situation, but in practice the fibers tend to fail sequentially starting with the weakest fiber, until the applied load cannot be supported leading to total fracture. Since the fibers are brittle and exhibit stochastic behavior, it is more appropriate to apply statistics to determine their ultimate strength. Duffy, et al. (1991) have pointed out that the strength distribution of the fibers needs to be incorporated into an analytical model for predicting the ultimate strength of the composite.

Equation 13 from Curtin, et al. (1993) and Curtin (1993) has been used to determine the composite's ultimate strength in terms of fiber properties.

$$\sigma_{cu} = V_f \left(\frac{2}{m+2} \right)^{\frac{1}{m+1}} \left(\frac{m+1}{m+2} \right) \left[\frac{\sigma_{fu}^m \tau L_f}{R \ln(2)} \right]^{\frac{1}{m+1}} \quad (13)$$

where L_f is the fiber gage length at which the strength was determined, m is the Weibull modulus of the fiber and σ_{fu} is the mean fiber strength

It is of interest to compare the above result to that found for a "dry" bundle containing only fibers and no matrix. The composite strength based on bundle ultimate strength, σ_{cub} , can be calculated, per Evans, et al. (1995), from

$$\sigma_{cub} = V_f \sigma_{fu} \left(\frac{L_f}{L_c} \right)^{\frac{1}{m}} e^{-\frac{1}{m}} \quad (14)$$

where L_c is the fiber bundle gage length and L_f is the fiber length used to determine σ_{fu} and m . Equation 14 uses the rule of mixtures to estimate the composite strength, σ_{cub} , with the product of the fiber volume fraction and the fiber bundle strength, σ_{fub} .

Evans (1989), as well as Evans and Marshall (1989), presented a model for predicting the composite ultimate strength based on weakest link statistics, incorporating the fiber Weibull modulus, m . The model is a modified bundle failure analysis which assumes failed fibers have no load bearing ability. The model of the modified bundle failure theory is presented in the following equation:

$$\sigma_{cubm} = V_f \sigma_{fub} e^{-\frac{1 - \left(1 - \frac{\tau x}{R \sigma_{fub}} \right)^{m+1}}{(m+1) \left[1 - \left(1 - \frac{\tau x}{R \sigma_{fub}} \right)^m \right]}} \quad (15)$$

The fiber bundle strength, σ_{fub} , is determined by iteratively solving the following equation:

$$\left(\frac{R \sigma_{fub}}{\tau x} \right)^{m+1} = \frac{A_o}{2\pi R L_c} \left(\frac{R \sigma_o}{\tau x} \right)^m \left[1 - \left(1 - \frac{\tau x}{R \sigma_{fub}} \right)^m \right]^{-1} \quad (16)$$

where τ is the interfacial shear stress as defined by equation 2 or 3, x is the saturated matrix crack spacing, R is the fiber radius, L_c is the composite gage length, and A_o is an area normalizing factor. The scale parameter, σ_o , is defined, according to Chulya, et al. (1991), by the following equation:

$$\sigma_o = \frac{\sigma_{fu}}{\Gamma\left(1 + \frac{1}{m}\right)} (2\pi R L_f)^{\frac{1}{m}} \quad (17)$$

Here L_f is the fiber gage length and Γ is Euler's gamma function, defined as:

$$\Gamma\left(1 + \frac{1}{m}\right) = \int_0^{\infty} t^{\left(1 + \frac{1}{m}\right)-1} e^{-t} dt \quad (18)$$

Cao and Thouless (1990) made an attempt to predict the ultimate strength of a ceramic composite with the application of two parameter Weibull statistics. Their theory assumed that the matrix is saturated with cracks. As a result, the initial linear elastic behavior and the nonlinear deformation associated with matrix cracking are not incorporated. Another simplifying assumption is that upon fracture of a fiber anywhere within the gage length of the composite, the fiber is unable to carry any load. Given the assumptions, the following equation is used to predict the ultimate strength of a ceramic composite:

$$\sigma_{cu} = V_f \Sigma \left(\frac{\Sigma R}{m(m+1)\tau L_c} \right)^{\frac{1}{m}} e^{-\frac{1}{m}} \quad (19)$$

where:

$$\Sigma = \left[\frac{A_o \sigma_o^m \tau (m+1)}{2 \pi R^2} \right]^{\frac{1}{m+1}} \quad (20)$$

As with the other theories in this section, this theory is based on fiber statistics, primarily the Weibull modulus and the scale parameter, and the variables are as defined in the statistical failure theories above.

5. RESULTS AND DISCUSSION

5.1. Microstructure

Figure 2 presents an SEM micrograph taken from the polished cross-section of the unidirectional composite indicating uniform fiber distribution and good matrix infiltration within the fiber tows. The fiber volume fraction in the composite is approximately 30%.

5.2 Mechanical Properties

In this section, the high temperature tensile test results are presented and compared with the theory to predict the mechanical behavior of the unidirectional fiber reinforced Hi-Nicalon/BSAS composite. Typical tensile stress-strain curves for the composite are presented in Fig. 3. All the specimens exhibited pseudo-toughness, or an ability to sustain progressive damage, from room temperature to 1200°C (2190°F) in air relative to monolithic BSAS. These temperatures were selected to represent potential service conditions. All the specimens tested shared linear elastic behavior, followed by matrix cracking region producing a limited nonlinear stress versus strain region.

The measured mechanical properties for all the short term static tensile tests for the composite at various temperatures are presented in Table I.

SEM micrographs of the fracture surfaces of the composite specimens after tensile tests at various temperatures are given in Fig. 4. Fibrous fracture surfaces are observed in specimens tested at 22, 800, 1000, and 1200°C (72, 1470, 1830, 2010, and 2190°F, respectively).

5.2.1 Modulus

Figure 5 and Table I show the Young's modulus of the composite as a function of temperature. The composite modulus decreases with increasing temperature. Monolithic BSAS specimens were tested at room temperature and reported by Bansal (1998). The monolithic material is similar to the matrix in the Hi-Nicalon/BSAS composite used for this work. The moduli of the constituents were used to determine the Young's modulus of the composite using the rule-of-mixtures, equation 1, at room temperature. The constituent moduli are $E_m = 96$ GPa (14 Mpsi) [Bansal (1998)] and $E_f = 270$ GPa (39 Mpsi) [Takeda, et al. (1995)]. There is excellent correlation between the measured and predicted values for the composite Young's modulus at room temperature, as shown in Figure 5.

5.2.2. Matrix Cracking and Interfacial Shear Properties

The effect of temperature on the proportional limit also was studied. It was assumed that the proportional limit, on a stress/strain curve, and the first matrix cracking stress were the same. The first matrix cracking stress is affected by various parameters. One of these parameters is the fiber/matrix interfacial shear strength. Other parameters are addressed later in this section. It has been noted by Kerans, et. al. (1989) that the interfacial shear strength is difficult to characterize with certainty.

An attempt was made at determining the matrix crack spacing in composites that have been loaded to the ultimate strength. Unfortunately, it was very difficult to locate through-the-composite, fiber bridged, regularly spaced cracks within the Hi-Nicalon/BSAS composite. Specimens tested at room temperature had some observable regularly spaced cracks. A mean crack spacing of 156 ± 36 μm (6.14 ± 1.42 mils) was measured. Using equation 2 the fiber/matrix interfacial shear stress, τ , is determined to be 4 MPa (600 psi). The low value for the interfacial shear stress is probably due to a lower than observed crack spacing. Specimens tested above ambient temperature did not have readily observable regularly spaced cracks.

Due to the difficulties in measuring matrix crack spacing, results from fiber push-in tests were used for determining the fiber/matrix interfacial shear properties in this work. An estimate of frictional sliding stress, τ , was determined using the model of Marshall and Oliver (1987), equation 3. The result of fiber push-in tests is a fiber/matrix interfacial shear stress, $\tau = 48.6 \pm 20.9$ MPa (7.05 ± 3.03 ksi). The fiber/matrix interfacial shear stress may be slightly overestimated by the model of Marshall and Oliver due to neglecting the Poisson expansion of the fibers.

The coefficient of thermal expansion (CTE) for the matrix and fibers are slightly different. The CTE value for Hi-Nicalon fibers, α_f , is $3.5 \times 10^{-6}/^\circ\text{C}$ ($1.9 \times 10^{-6}/^\circ\text{F}$) from 25 to 500°C (77-930°F) according to data from its producer, Nippon Carbon Company. The CTE value for BSAS, α_m , is $5.28 \times 10^{-6}/^\circ\text{C}$ ($2.93 \times 10^{-6}/^\circ\text{F}$) from room temperature to 1200°C (2190°F) according to Bansal (1998). It is assumed that the thermal expansion coefficients of the constituents remain constant for the temperature range used in this work. The different thermal expansion coefficients of the constituents results in residual stresses within the composite at temperatures other than the processing temperature. The processing temperature, assumed to be approximately 1300°C (2400°F), is used as the reference temperature at which there are no residual stresses due to the CTE mismatch within the composite. Equation 6 is used to determine the residual stress within the matrix. The Poisson's ratio is assumed to be the same for the fiber and the matrix at a mean value of $\nu = \nu_f = \nu_m = 0.22$.

The first matrix cracking stress values at the proportional limit are illustrated in Figure 6 and Table I. In addition, Figure 6 shows predicted values from the ACK theory and the Marshall and Cox theory combined with the McCartney theory at room temperature. The matrix fracture surface energy, γ_m , is assumed to be a conservative 5 J/m² (0.03 in· lbf/in²). The value for the matrix crack surface energy is taken from Wachtman Jr. (1996) who showed ceramics to typically vary from 5 to 50 J/m² (0.03 to 0.29 in· lbf/in²).

Looking at Figure 6 we find that the estimated values for the first matrix cracking stress by the ACK theory estimates the room temperature first matrix cracking stress fairly accurately while accounting for residual stresses and assuming a frictional fiber/matrix interface. On the other hand, by accounting for the residual stresses the Marshall and Cox theory combined with the McCartney theory results in a conservative prediction for the first matrix cracking stress.

5.2.3 Hi-Nicalon Fiber Properties

Hi-Nicalon fibers were extracted from the Hi-Nicalon/BSAS composite, by dissolving away the matrix in hydrofluoric acid, and tensile tested at room temperature [Bansal (1998)]. The room temperature properties include mean ultimate strength, σ_{fu} , of 2.38 GPa (345 ksi); with one standard deviation of ± 0.40 GPa (58 ksi); and a Weibull modulus, m , of 5.6. Figure 7 presents a typical two-parameter Weibull plot with $\ln(\ln(1/(1-P_f)))$ versus the fiber ultimate strength for the extracted Hi-Nicalon fibers. The same figure illustrates the 90% confidence bounds as determined using the ASTM (1995) standard designation C 1239-94a. The Weibull modulus is determined by numerically solving the equations for the maximum likelihood method as presented in the standard.

5.2.4 Composite Ultimate Tensile Strength

The ultimate strengths of these composites are primarily dependent on fiber properties. The strength properties of Hi-Nicalon fibers were discussed in the previous section. The ultimate strength of individual specimens is presented in Table I. The mean ultimate tensile strength of the composites are plotted as a function of temperature in Figure 8. The plot includes the theoretical estimates using constituent properties at room temperature. To reiterate, the test temperatures were room temperature, 800°, 1000°, 1100°, and 1200°C (1470, 1830, 2010, and 2190°F, respectively). Figure 8 indicates a steady drop in the ultimate strength of the composite from room temperature to 1200°C (2190°F).

It can be observed in Figure 8 that the rule of mixtures, equation 12, over-predicts the ultimate strength. It was mentioned in the previous section that this approach assumes that all the fibers are intact just prior to the composite ultimate strength. The rule of mixtures does not account for the brittle nature of the reinforcing fibers and the corresponding variance in the strength of the fibers. As a result, the rule of mixtures assumes ideal conditions, producing optimistic strength values relative to the experimentally derived measurements of the composites.

Since the fibers are brittle and exhibit linear elastic behavior with a significant variance in strength, relative to metals or other common structural materials, it is more appropriate to apply statistics to determine the ultimate strength. The other theories in this work apply Weibull statistics in an attempt to increase the accuracy in predicting the composite ultimate strength.

Curtin's (1993) theory, equation 13, produces optimistic values for the ultimate strength that are significantly higher than the measured ultimate strengths. Evans', et al. (1995) theory, equation 14, estimates the ultimate strength of the Hi-Nicalon/BSAS composite at room temperature with good accuracy. Evans' (1989) model, equation 15, also produces a very accurate estimate of the composite ultimate strength of the Hi-Nicalon/BSAS. For Evans' (1989) model the fiber bundle strength, σ_{fub} , was determined to be 2.28 GPa (331 ksi) by iteratively solving equation 16 and the scale parameter, σ_o , was determined to be 220 MPa (32 ksi) using equation 17. The area normalizing factor, A_o , was equal to 1.0 m² (1550 in²). The theory from Cao and Thouless (1990), equation 19, under estimates the composite ultimate strength by 25%. The same scale parameters, σ_o , calculated for the modified fiber bundle theory of Evans (1989), was used for this theory.

The application of the mean fiber strength and the fiber Weibull modulus does predict the ultimate strength of the composite with increased accuracy. Increasing the number of specimens per test should show more accurate results when applying statistics. Lastly, the mean strengths and Weibull moduli for the fibers were generated by testing individual fibers. Hill and Okoroafor (1995) have observed a reduction in strength of fiber bundles due to inter-fiber friction. This inter-fiber friction may be causing some of the reduction in strength of the experimentally derived composite data relative to the theoretical values derived from individually tested fibers. On an interesting note, Cox, Marshall, and Thouless (1989) found that the fracture of composites is not greatly influenced by the breadth of the fiber strength distribution. Overall, the theories incorporating the scatter in fiber strength improved the predictions of the composite ultimate strength.

6. SUMMARY AND CONCLUSIONS

Tensile mechanical properties of unidirectional Hi-Nicalon/BSAS composites have been measured at various temperatures up to 1200°C (2190°F) in air. The applicability of currently available micromechanical models in predicting the various mechanical properties of this CMC has also been tested.

The composite exhibited progressive fracture in short term static tensile tests at all test temperatures. The Young's modulus shows a slight decrease as the test temperature was increased from room temperature to 800°C (1470°F) but decreased at a greater rate above 800°C (1470°F). The rule of mixtures gives a good approximation of the composite modulus at room temperature.

The first matrix cracking stress showed a minor decrease as temperatures increased from room temperature to 1200°C (2190°F). The ACK theory, with the assumption of a frictional fiber/matrix interface and accounting for residual stresses, produces a good approximation for the composite first matrix cracking stress at room temperature. The Marshall and Cox theory combined with the McCartney theory underestimates the first matrix cracking stress while accounting for residual stresses at room temperature. The testing and analysis of the fiber/matrix interfacial shear strength, especially above ambient temperature, requires further study. A better understanding of the fiber/matrix interfacial properties would help improve predictions for the first matrix cracking stress.

The ultimate strength showed a drop from room temperature to 1200°C (2190°F). The theories of Evans et al. (1995) and Evans (1989) gave the best estimates of the room temperature ultimate strength relative to other theories evaluated in this work.

REFERENCES

- American Society for Testing and Materials, "ASTM Designation: C 1239-94a: Standard Practice for Reporting Uniaxial Strength Data and Estimating Weibull Distribution Parameters for Advanced Ceramics," 1995 Annual Book of ASTM Standards, Refractories; Carbon and Graphite Products; Activated Carbon; Advanced Ceramics, Vol. 15.01. ASTM, Philadelphia, PA.
- Aveston, J., Cooper, G. A., and Kelly, A., "Single and Multiple Fracture in the Properties of Fiber Composites," Conference Proceedings, National Physical Laboratory, Guildford. IPC Science and Technology Press Ltd., Surrey, England, 1971, pp. 15-26.
- Bansal, N. P., "Effects of HF Treatments On Tensile Strength of Hi-Nicalon Fibres," Journal of Materials Science, Vol. 33, 1998, pp. 4287-4295.
- Bansal N. P. and Eldridge, J. I., "Hi-Nicalon Fiber-Reinforced Celsian Matrix Composites: Influence of Interface Modification," Journal Materials Research, Vol. 13, No. 6, pp. 1530-1537, 1998.
- Bansal, N. P., "Strong and Tough Hi-Nicalon Fiber-Reinforced Celsian Matrix Composites," Journal of the American Ceramic Society, Vol. 80, No. 9, pp. 2407-2409, 1997.
- Bansal, N. P., "Solid State Synthesis and Properties of Monoclinic Celsian," NASA Technical Memorandum 107355, 1998.
- Bansal, N. P., "CVD SiC Fiber-Reinforced Barium Aluminosilicate Glass-Ceramic Matrix Composites," Materials Science and Engineering A, Vol. 220, Nos. 1-2, pp. 129-139 1996.
- Bansal, N. P. and Setlock, J. A., "Processing of Small Diameter Fiber-Reinforced Celsian Composites," NASA Technical Memorandum 107356, 1996.
- Bansal, N. P.; McCluskey, P.; Linsey, G.; Murphy, D.; and Levan, G.; "Nicalon Fiber-Reinforced Celsian Glass-Ceramic Matrix Composites," Proceedings of Annual HITEMP Review, Cleveland, OH, Oct. 23-25, 1995. NASA Conference Publication 10178, Vol. III, pp. 41-1 to 41-14, 1995.
- Bansal, N. P., "Method of Producing a Ceramic Fiber-Reinforced Glass-Ceramic Matrix Composite," U. S. Patent, 5,281,559, Jan. 25, 1994.
- Bansal, N. P., "Ceramic Fiber-Reinforced Glass-Ceramic Matrix Composite," U. S. Patent 5,214,004, May 25, 1993.
- Bergman, B., "On the Estimation of the Weibull Modulus," Journal of the Materials Science Letters, Vol. 3, 1984.
- Budiansky, B., Hutchinson, J. W., and Evans, A. G., "Matrix Fracture In Fiber Reinforced Ceramics," Journal of the Mechanics and Physics of Solids, Vol. 34, 1986, pp. 167-189.
- Cao, H. and Thouless, M. D., "Tensile Tests of Ceramic-Matrix Composites: Theory and Experiment," Journal of the American Ceramic Society, Vol. 73, No. 7, 1990.
- Chulya, A., Gyekenyesi, J. P., and Bhatt, R. T., "Mechanical Behavior of Fiber Reinforced SiC/RBSN Ceramic Matrix Composites: Theory and Experiment," NASA Technical Memorandum 103688, 1991.

- Constance, J., "Industry Turns to Ceramic Composites," Aerospace America, Mar., 1990.
- Cox, B. N., Marshall, D. B., and Thouless, M. D., "Influence of Statistical Fiber Strength Distribution on Matrix Cracking in Fiber Composites," Acta Metallurgica, Vol. 37, No. 7, 1989, pp. 1933-1943.
- Curtin, W. A., Eldridge, J. I., and Srinivasan, G. V., "New Silicon Carbide/Reaction Bonded Silicon Carbide Ceramic Matrix Composite," Journal of the American Ceramic Society, Vol. 76, No. 9, 1993.
- Curtin, W. A., "Ultimate Strengths of Fibre-Reinforced Ceramics and Metals," Composites, Vol. 24, No. 2, 1993.
- Danchaivijit, S. and Shetty, D. K., "Matrix Cracking In Ceramic-Matrix Composites," Journal of the American Ceramic Society, Vol. 76, No. 10, 1993.
- Dix, D. M. and Petty, J. S., "Aircraft Technology Gets A Second Wind," Aerospace America, Jul., 1990.
- Drascovich, B. S., "Fibers for Turbines," CFCC News, Summer, 1993.
- Duffy, S. F., Chulya, A., and Gyekenyesi, J. P., "Structural Design Methodologies for Ceramic-Based Material Systems," NASA Technical Memorandum 103097, 1991.
- Duffy, S. F. and Gyekenyesi, J. P., "Reliability and Life Prediction of Ceramic Composite Structures at Elevated Temperatures," in High Temperature Mechanical Behavior of Ceramic Composites, S.V. Nair and K. Jakus, eds., pp. 471-515, Butterworth-Heinemann, Boston, 1995.
- Eldridge, J. I., "Desktop Fiber Push-out Aparatus," NASA Technical Memorandum 105341, 1991.
- Evans, A. G., "The Mechanical Performance of Fiber-Reinforced Ceramic Matrix Composites," Materials Science and Engineering, A107, 1989.
- Evans, A. G. and Marshall, D. B., "The Mechanical Behavior of Ceramic Matrix Composites," Acta Metallurgica, Vol. 37, No. 10, 1989, pp. 2567-2583.
- Evans, A. G., Zok, F. W., and Mackin, T. J., "The Structural Performance of Ceramic Matrix Composites," High Temperature Mechanical Behavior of Ceramic Composites, ed. Nair, S. V. and Jakus, K., Boston: Butterworth-Heinemann, 1995, pp. 3-84.
- Gyekenyesi, J. Z. and Jaskowiak, M. H., "High Temperature Mechanical Characterization and Analysis of Al_2O_3/Al_2O_3 Composites," NASA Technical Memorandum 1999-208855, 1999.
- Gyekenyesi, J. Z., "High Temperature Mechanical Characterization of Ceramic Matrix Composites," Ph.D. Thesis, Cleveland State University, 1998.
- Hill, R. and Okoroafor, E. U., "Weibull Statistics Of Fibre Bundle Failure Using Mechanical and Acoustic Emission Testing: The Influence of Interfibre Friction," Composites, Vol. 26, No. 10, 1995.
- Holmes, J.W. and Wu, X., "Elevated Temperature Creep Behavior of Continuous Fiber-Reinforced Ceramics," in High Temperature Mechanical Behavior of Ceramic Composites, ed. Nair, S. V. and Jakus, K., pp. 193-259, Butterworth-Heinemann, Boston, 1995.
- Kimber, A. C. and Keer, J. G., "On the Theoretical Average Crack Spacing In Brittle Matrix Composites Containing Continuous Aligned Fibers," Journal of Materials Science Letters, Vol. 1, 1982.
- King, J. E., "Failure In Composite Materials," Metals and Materials, Dec., 1989.
- Kerans, R. J., Hay, R. S., Pagano, N. J., Parthasarathy, T. A., "The Role of the Fiber-Matrix Interface in Ceramic Composites," Ceramic Bulletin, Vol. 68, No. 2, 1989.
- Levine, S. R., "Ceramics and Ceramic Matrix Composites - Aerospace Potential and Status," American Institute of Aeronautics and Astronautics report AIAA-92-2445-CP, 1992.
- Marshall, D. B. and Cox, B. N., "A J-Integral Method for Calculating Steady-State Matrix Cracking Stresses In Composites," Mechanics of Materials, Vol. 7, 1988, pp. 127-133.
- Marshall, D. B. and Oliver, W. C., "Measurement of Interfacial Mechanical Properties in Fiber-Reinforced Ceramic Composites," Journal of the American Ceramic Society, Vol. 70, No. 8, pp. 542-548, 1987.
- McCartney, L. N., "Mechanics of Matrix Cracking in Brittle-Matrix Fiber-Reinforced Composites," Royal Society of London, Proceedings, Series A, Vol. 409, 1987, pp. 329-350.
- Sheppard, L. M., "Enhancing Performance of Ceramic Composites," Ceramic Bulletin, Vol. 71, No. 4, 1992.
- Shimansky, R. A., "Effect of Interfaces On Continuous Fiber-Reinforced Brittle Matrix Composites," Ann Arbor, Michigan: University Microfilms International, 1989.
- Studt, T., "Breaking Down Barriers for Ceramic Matrix Composites," R&D Magazine, Aug., 1991.
- Takeda, M.; Sakamoto, J.; Saeki, S.; Imai, Y.; and Ichikawa, H.: "High Performance Silicon Carbide Fiber Hi-Nicalon for Ceramic Matrix Composites," Ceramic Engineering and Science Proceedings, Vol. 16, No. 4, pp. 37-44, 1995.
- Wachtman Jr., Mechanical Properties of Ceramics, New York: John Wiley & Sons, Inc., 1996.
- Warren, R., "Overview," Ceramic-Matrix Composites, ed. R. Warren. New York: Chapman and Hall, 1992. p.5

- Weibull, W., "The Phenomenon of Rupture in Solids," *Ingeniors Ventenskaps Akademien Handlinger*, No. 153, 1939, pp. 5-55.
- Woodford, D. A., Van Steele, D. R., Brehm, J. A., Timms, L. A., and Palko, J. E., "Testing the Tensile Properties of Ceramic-Matrix Composites," *JOM*, Vol. 45, No. 5, May, 1993.
- Worthem, D. W. and Lewinsohn, C. A., "Effect of Specimen Design on the Tensile Properties of Ceramic Matrix Composites," Proceedings of 4th Annual HITEMP Review, Cleveland, OH, Oct. 29-30, 1991. NASA Conference Publication 10082, pp. 49-1 to 49-10, 1991.
- Worthem, D. W., "Flat Tensile Specimen Design for Advanced Composites," NASA Contractor Report 185261, Nov., 1990.
- Zweben, C., "Advanced Composites In Spacecraft and Launch Vehicles," *Launchspace*, Jun./Jul., 1998.

Table I. Tensile property data for Hi-Nicalon/BSAS composite at various temperatures in air.

T (°C)	E _c (GPa)	σ _y (MPa)	ε _y (%)	σ _u (MPa)	ε _u (%)
22	156	81	0.052	574	0.455
	153	112	0.073	603	0.441
800	129	74	0.057	444	0.446
	135	62	0.046	452	0.383
1000	102	77	0.076	505	
	109	62	0.053	456	0.397
1100	94	98	0.105	399	0.433
	89	86	0.096	402	0.523
1200	78	59	0.074	382	
	68	137	0.204	357	0.806

fiber volume fraction: 0.3
 fiber orientation: 0°
 no. of plies: 12
 gage length: 25 mm

T – test temperature
 E_c – Young's modulus
 σ_y – first matrix cracking stress
 ε_y – strain at σ_y
 σ_u – ultimate strength
 ε_u – strain at σ_u

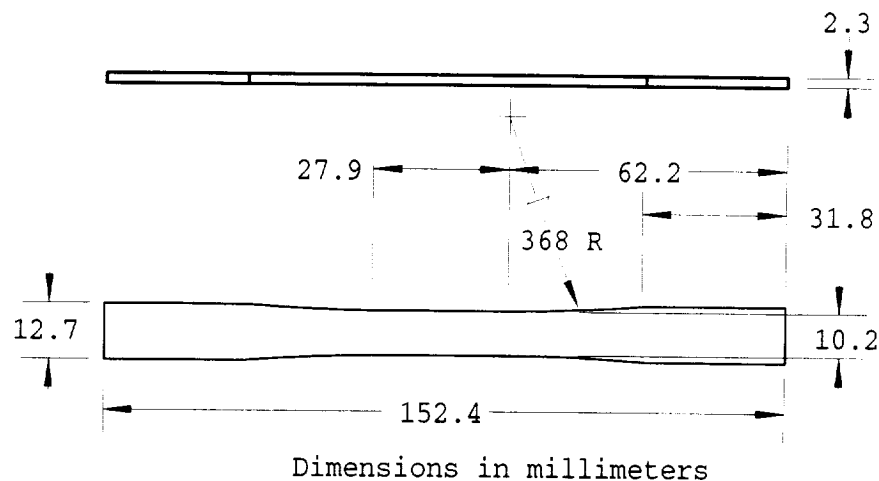


Figure 1. Contoured tensile specimen.

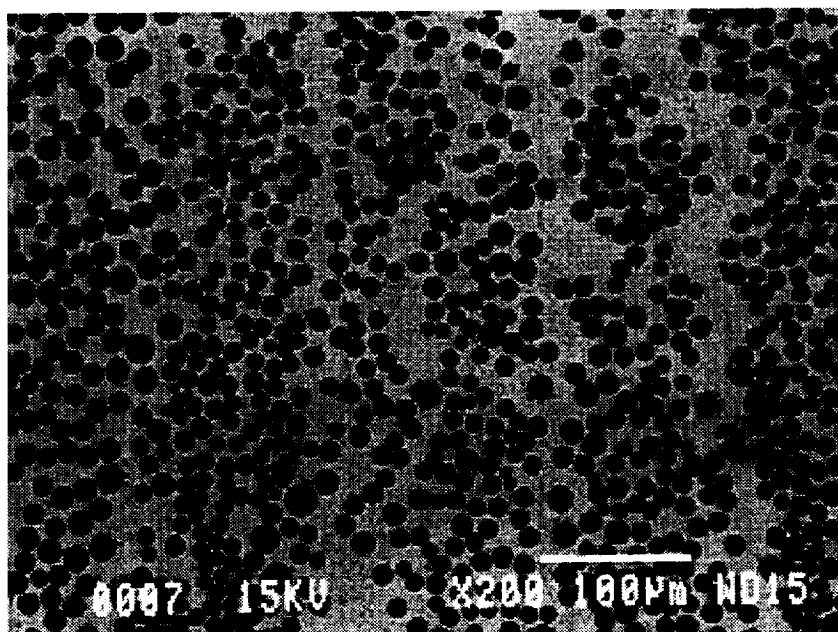


Figure 2. SEM micrographs showing polished cross-section of unidirectional celsian matrix composite reinforced with BN/SiC-coated Hi-Nicalon fibers.

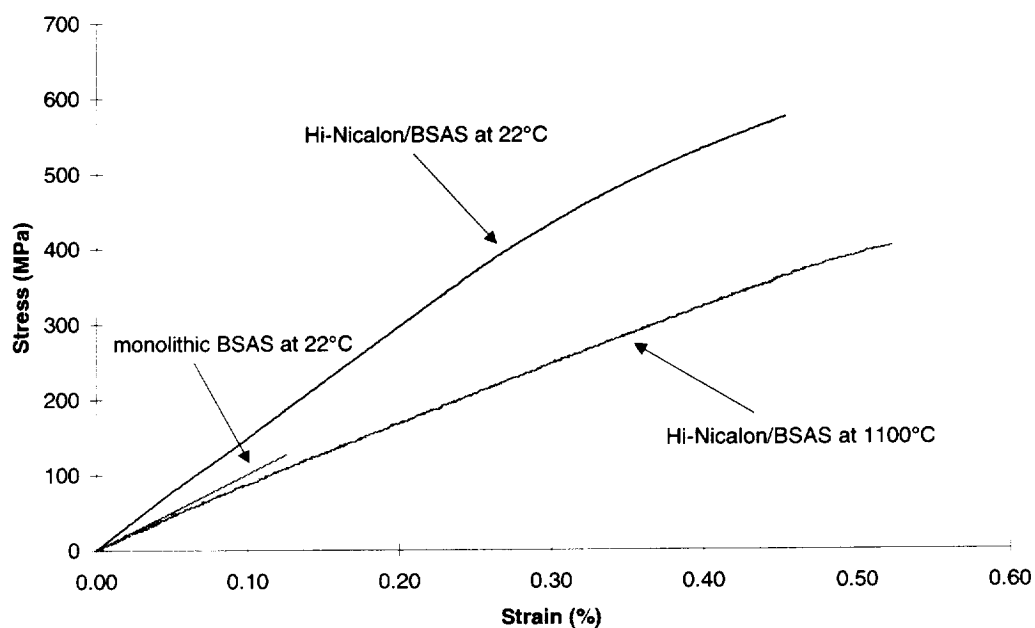
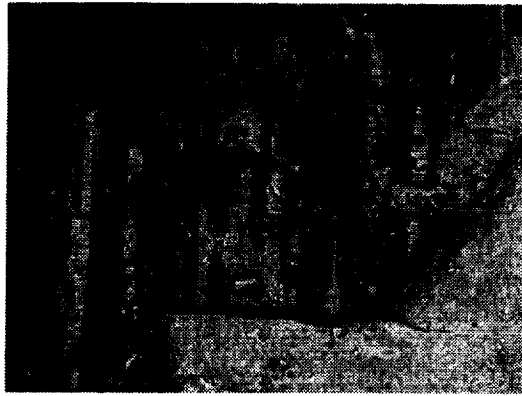


Figure 3. Tensile stress-strain curves of unidirectional Hi-Nicalon/BSAS composites at 22 and 1100°C in air. The stress-strain curve for monolithic BSAS at 22°C is also included for comparison.



22°C



800°C



1200°C

Figure 4. SEM micrographs showing fracture surfaces of unidirectional Hi-Nicalon/BSAS composites after tensile testing at various temperatures. Fibrous fractures are evident.

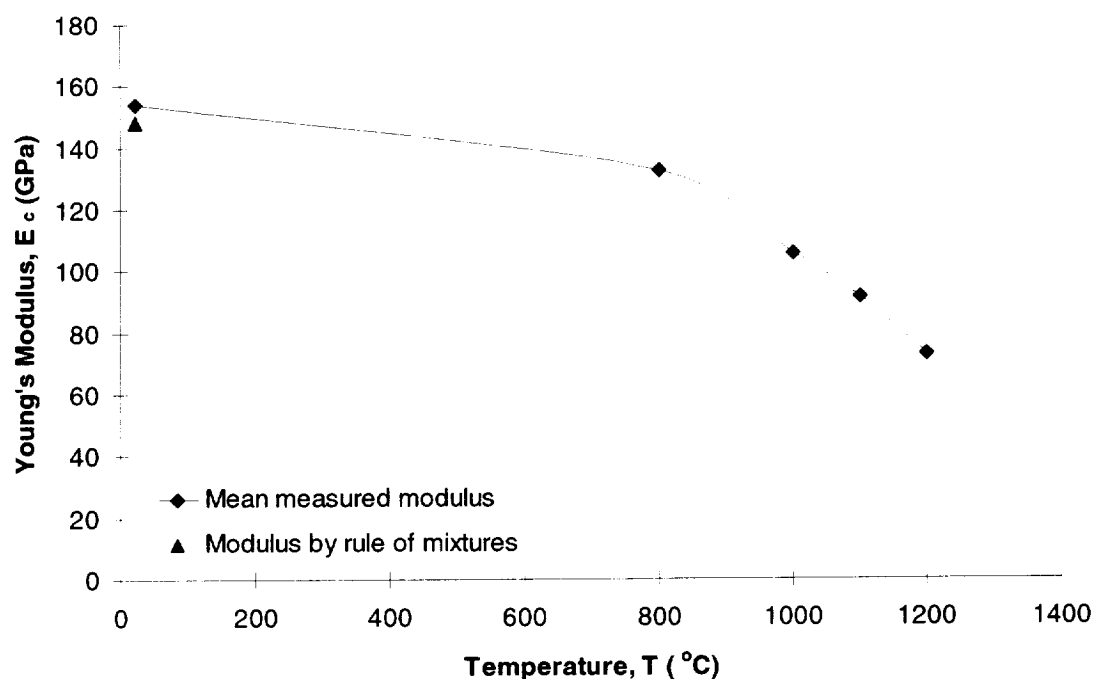


Figure 5. Tensile Young's modulus of Hi-Nicalon/BSAS composites as a function of temperature in air.

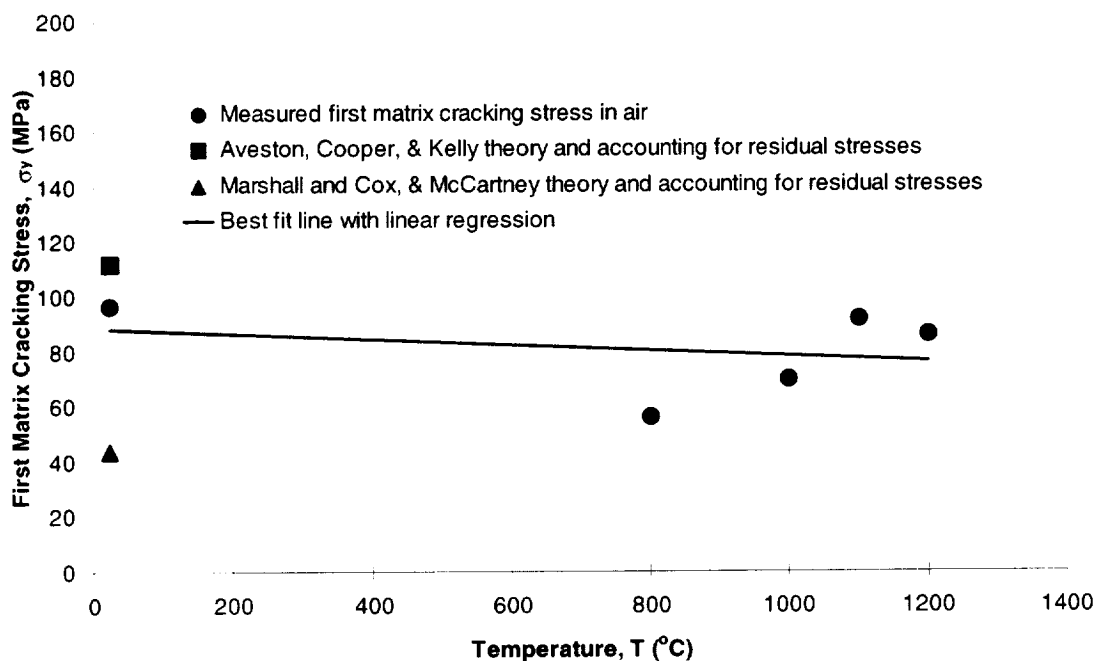


Figure 6. Mean first matrix cracking stress of Hi-Nicalon/BSAS composites in air as a function of temperature. Values estimated from various micromechanical models at room temperature are also shown.

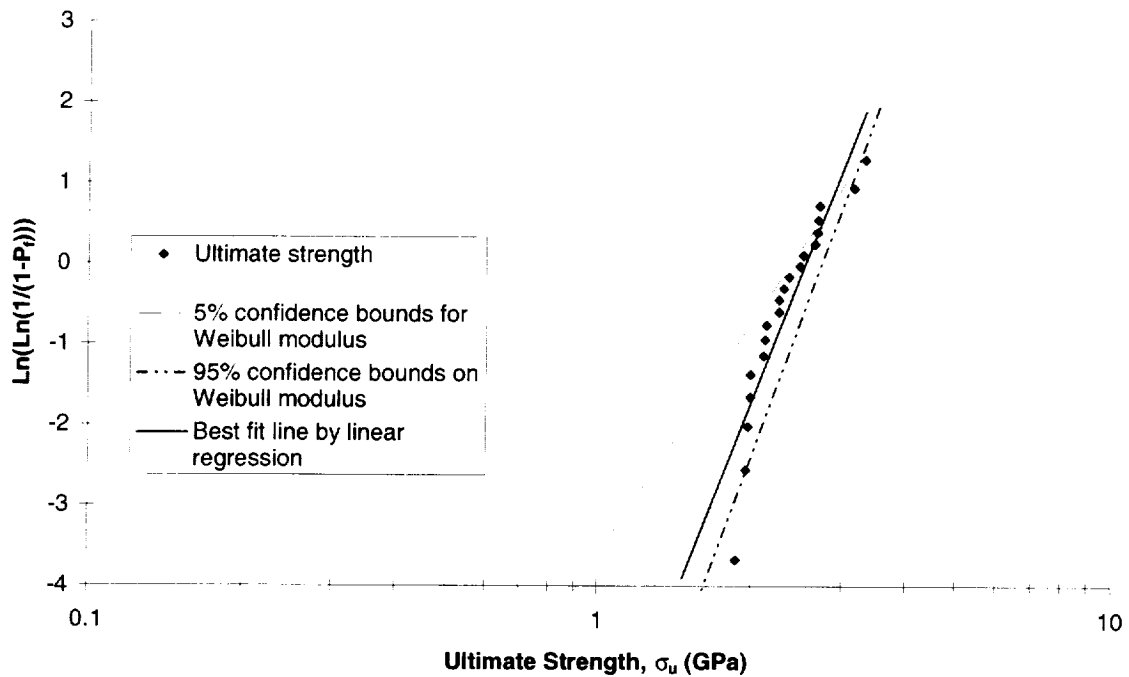


Figure 7. Two parameter Weibull plot for Hi-Nicalon fibers tensile tested at 22°C. Ninety percent confidence bounds determined as per ASTM (1995) standard designation C 1239-94a.

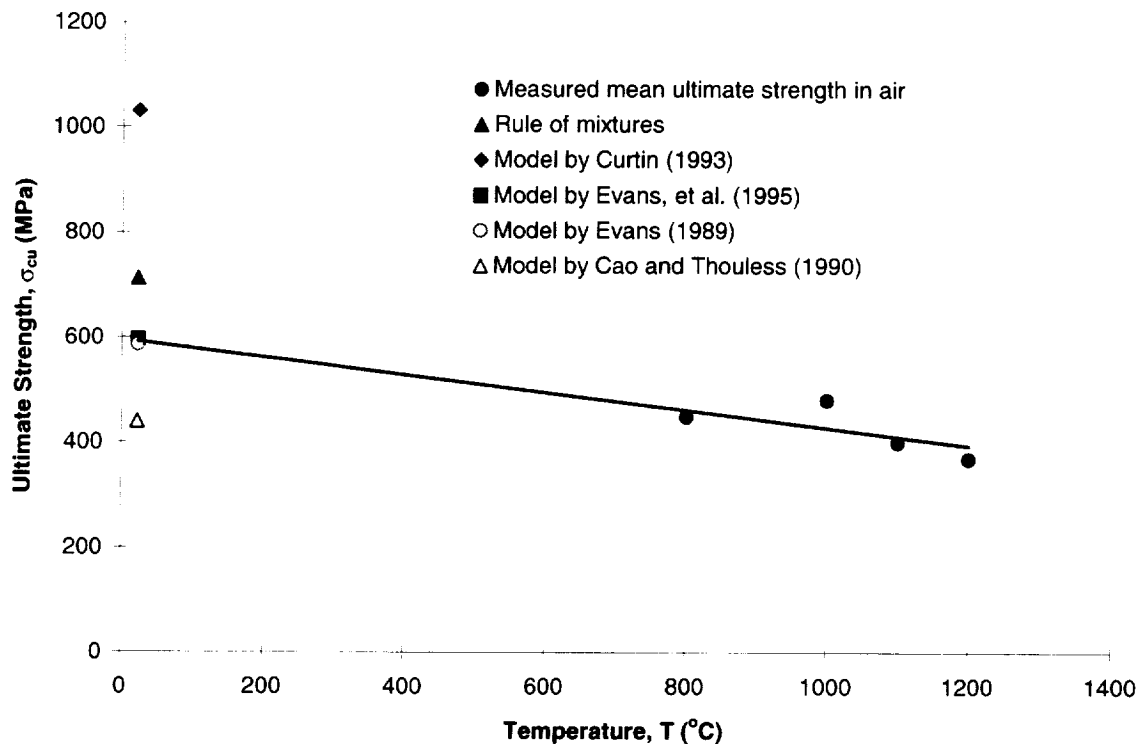


Figure 8. Temperature dependence of the tensile ultimate strength in air. Values estimated from various micromechanical models at room temperature are also shown. The models use property data from fibers extracted from the composite.

REPORT DOCUMENTATION PAGE

Form Approved

OMB No. 0704-0188

Public reporting burden for this collection of information is estimated to average 1 hour per response, including the time for reviewing instructions, searching existing data sources, gathering and maintaining the data needed, and completing and reviewing the collection of information. Send comments regarding this burden estimate or any other aspect of this collection of information, including suggestions for reducing this burden, to Washington Headquarters Services, Directorate for Information Operations and Reports, 1215 Jefferson Davis Highway, Suite 1204, Arlington, VA 22202-4302, and to the Office of Management and Budget, Paperwork Reduction Project (0704-0188), Washington, DC 20503.

1. AGENCY USE ONLY (Leave blank)**2. REPORT DATE**

July 2000

3. REPORT TYPE AND DATES COVERED

Technical Memorandum

4. TITLE AND SUBTITLE

High Temperature Tensile Properties of Unidirectional Hi-Nicalon/Celsian Composites In Air

5. FUNDING NUMBERS

WU-523-75-13-00

6. AUTHOR(S)

John Z. Gyekenyesi and Narottam P. Bansal

7. PERFORMING ORGANIZATION NAME(S) AND ADDRESS(ES)National Aeronautics and Space Administration
John H. Glenn Research Center at Lewis Field
Cleveland, Ohio 44135-3191**8. PERFORMING ORGANIZATION
REPORT NUMBER**

E-12333

9. SPONSORING/MONITORING AGENCY NAME(S) AND ADDRESS(ES)National Aeronautics and Space Administration
Washington, DC 20546-0001**10. SPONSORING/MONITORING
AGENCY REPORT NUMBER**

NASA TM-2000-210214

11. SUPPLEMENTARY NOTESJohn Z. Gyekenyesi, Ohio Aerospace Institute, 22800 Cedar Point Road, Brook Park, Ohio 44142; and
Narottam P. Bansal, NASA Glenn Research Center. Responsible person, John Z. Gyekenyesi, organization code 5130,
(216) 433-8184.**12a. DISTRIBUTION/AVAILABILITY STATEMENT**Unclassified - Unlimited
Subject Categories: 39, 24, and 27

Distribution: Nonstandard

This publication is available from the NASA Center for AeroSpace Information, (301) 621-0390.

12b. DISTRIBUTION CODE**13. ABSTRACT (Maximum 200 words)**

High temperature tensile properties of unidirectional BN/SiC-coated Hi-Nicalon SiC fiber reinforced celsian matrix composites have been measured from room temperature to 1200 °C (2190 °F) in air. Young's modulus, the first matrix cracking stress, and the ultimate strength decreased from room temperature to 1200 °C (2190 °F). The applicability of various micromechanical models, in predicting room temperature values of various mechanical properties for this CMC, has also been investigated. The simple rule of mixtures produced an accurate estimate of the primary composite modulus. The first matrix cracking stress estimated from ACK theory was in good agreement with the experimental value. The modified fiber bundle failure theory of Evans gave a good estimate of the ultimate strength.

14. SUBJECT TERMS

Ceramic matrix composites; Glass ceramics; Tensile test; High temperature

15. NUMBER OF PAGES

29

16. PRICE CODE

A03

**17. SECURITY CLASSIFICATION
OF REPORT**

Unclassified

**18. SECURITY CLASSIFICATION
OF THIS PAGE**

Unclassified

**19. SECURITY CLASSIFICATION
OF ABSTRACT**

Unclassified

20. LIMITATION OF ABSTRACT

